Energy 93 (2015) 2337–2350

Contents lists available at ScienceDirect

Energy

journal homepage: www.elsevier.com/locate/energy

A bottom-up and procedural calibration method for building energy simulation models based on hourly electricity submetering data

Ying Ji, Peng Xu*

School of Mechanical Engineering, Tongji University, Shanghai, 201804, China

ARTICLE INFO

Article history:
Received 12 August 2015
Received in revised form
24 September 2015
Accepted 10 October 2015
Available online 19 November 2015

Keywords:
Building energy simulation models
Calibration
Submetering data
Cooling/heating load

ABSTRACT

BESMs (building energy simulation models) play an important role in the design, optimization and retrofit of buildings. Developing a BESM is relatively simple in the building design phase because nearly all inputs are known from design parameters. However, in the building operation phase, developing and calibrating a BESM becomes difficult because all operating parameters must be adjusted according to real-time data. All of these parameters are difficult to measure, and they vary over time. Existing calibration methods of BESMs, which involve hundreds of input parameters, lack standard procedures and require specialized engineers. Engineers must randomly adjust input parameters until the output energy use matches measured energy use. To solve the problem above, a new calibration approach with a detailed procedure is proposed in this paper. This approach relies on electricity submetering data and HVAC (Heating, Ventilation and Air Conditioning) cooling/heating loads. These data are becoming more available in commercial buildings. A case study is demonstrated in a large commercial building with satisfying results. The CV (coefficient of variation) and MBE (mean bias error) of the total hourly electricity consumption simulation, excluding HVAC, are 4% and 3%, respectively. The CVs of an HVAC system are 12% (chiller), 6% (pump) and 5% (fan), and the MBEs are 10% (chiller), 5% (pump) and 4% (fan).

1. Introduction

Buildings consume about one-third of the global energy consumption. In the United States, Europe and China, building sector energy use accounted for 41.3% (2010), 40% (2010) and 28% (2012) of total energy use [1–5]. Thus, the retrofitting and energy efficiency management of existing commercial buildings are particularly important. More and more BESMs (building energy simulation models) are built to simulate existing buildings in operation, rather than buildings in design. Calibrating the models with building operation data is becoming an important issue.

BESMs can be divided into three categories. 1) Black-box models (data-driven models) are simple mathematical or statistical models resulting from long-term historical data training. These models have high requirements for the quality and quantity of data, but lack physical meaning, and they include traditional regression models [6–8], ANN (artificial neural network) models [9–11] and SVM (support vector machine) models [12–14]. 2) Grey-box models differ from black-box approaches in that they use certain parameters identified from physical system models, such as decision tree models [15,16] and Fourier series models [17–19]. 3) White-box models (law-driven models) [20–22] use fully descriptive law-driven models of building systems and tune the various inputs to match the measured data. Those approaches provide the most detailed prediction of building performance given the availability of high-quality input data. In this modeling field, there is not only a variety of software tools supplied to users, such as DOE-2, ESP-r, Energyplus and TRNSYS [23–26], but also some specifications, such as Annex 53, IPMVP and ASHRAE Guideline 14 [27–29] and a comprehensive and systematic specifications and textbook written by Jan L.M. Hensen and Roberto Lamberts [30]. However, extensive work experience and professional operator skills are required to calibrate this type of model.

Building BESMs with high accuracy and applicability have significant benefits in the following fields: 1) energy consumption prediction, 2) energy savings calculation and 3) baseline establishment. Setting up a BESM is relatively easy in the building design phase because nearly all of the inputs are known from design parameters. However, simulating buildings in operation is difficult because of hundreds of unknown variables, such as occupancy and

* Corresponding author. Tel.: +86 021 65989750.
E-mail address: xupeng@tongji.edu.cn (P. Xu).

http://dx.doi.org/10.1016/j.energy.2015.10.109
0360-5442/

Nomenclature

CV	coefficient of variability (%)
MRE	mean relative error (%)
E	electricity energy use (kWh)
P_i	instantaneous power (W or kW)
τ	data collection cycle for instantaneous power (min)
n	the total number of chillers
t	data collection cycle for temperature and water flow rate (min)
C	the specific heat of water (4.187 kJ/(kg °C))
M_j	chilled water flow rate (kg/s)
ΔT_j	the temperature difference between chilled water (hot water) inlet and outlet (°C)
E_L	lighting-plug submeter energy use (kWh)
E_P	power submeter energy use (kWh)
α_m, β_m, δ_n, η_n, γ_m, μ_n, κ_n	coefficients of Fourier series model frequencies
ω_m	Fourier frequency for day
ω_n	Fourier frequency for hour
d	day of year
h	hour of day
$\overline{T}$	the indoor mean temperature (°C)
T_i	the temperature of the ith measurement point (°C)
V_i	the volume of zone i (m^3)
$\overline{H}$	the indoor mean absolute humidity (g/kg)
H_i	the absolute humidity of the ith measurement point (g/kg)
T_{el}	leaving chilled water temperature (°C)
T_{ce}	entering condenser water temperature (°C)
COP	coefficient of performance
PLR	the ratio of actual cooling load to rated cooling load
$PPLR$	the ratio of actual water flow rate to rated flow rate
$FPLR$	the ratio of actual air flow rate to rated flow rate
$c_0 \sim c_3$, $p_0 \sim p_3$, $f_0 \sim f_3$, $m_0 \sim m_5$, $n_0 \sim n_5$	parameters of models
P_{pump}	actual power of pump (W or kW)
P_{pl}	performance coefficient of pump
P_{design}	rated power of pump (W or kW)
Q_{actual}	actual cooling load (W or kW)
ρ	the density of water (1000 kg/m^3)
ΔT_{actual}	the actual temperature difference between chilled water inlet and outlet (°C)
F_{design}	rated flow rate of chilled pump (m^3/h)
$\Delta T'_{actual}$	the actual temperature difference between chilling water inlet and outlet (°C)
F'_{design}	rated flow rate of chilling pump (m^3/h)
P_{fan}	actual power of fan (W or kW)
F_{pl}	performance coefficient of fan
F_{design}	rated power of fan (W or kW)
C'	the specific heat of air (1.005 kJ/(kg °C))
ρ'	the density of air (1.2 kg/m^3)
ΔT_{air}	the actual temperature difference between supply air and indoor air (°C)
$F_{airdesign}$	rated flow rate of terminal fan (m^3/h)
$M_{chilling}$	actual flow rate of chilling water (m^3/h)
$P_{chiller}$	power of chiller (W or kW)
$\Delta T'_{air}$	the actual air temperature difference between cooling tower inlet and outlet (°C)
ΔH_{actual}	the actual air enthalpy difference between cooling tower inlet and outlet (kJ/kg)
$F'_{airdesign}$	rated flow rate of cooling tower fan (m^3/h)
E_{Mi}	measured energy use data of ith data point (kWh)
E_{Pi}	calculated energy use data of ith data point (kWh)
N	total number of data points

internal load schedule. The difficulty of BESM calibration in existing buildings results from three key problems: 1) Non-unique solutions. The calibration of forward BESM programs, involving hundreds of input parameters, is a highly under-determined problem which yields multiple non-unique solutions [31–33]; 2) Inaccurate results. Forecasting building energy consumption is difficult due to the complexity of the system inside the building. For example, the infiltration air exchange rate varies from day to day and the occupancy schedule does not necessary fit with fixed weekday and weekend patterns as described in input schedules. Numerous studies [34–36] have indicated that the discrepancies between BESM model predictions and the actual measured building energy use are often significant (up to 100% differences); 3) Time cost. The calibration of the BESM of an existing commercial building still requires much time, even if the engineers are professional and highly experienced [37].

In most current prevailing engineering practices [38,39], the first step in building a BESM is to collect the building's monthly total energy use from the electricity bills. Next, engineers constantly adjust the input parameters of the BESM until the simulated total energy consumption matches the measured data, which gives rise to a “non-unique solution”, because different input setups can generate the same output solutions. Many researches are conducted on calibrating whole building energy models using hourly measured data (or called short-time scale data), with two main issues still unsolved in this field [40–44]. 1) Electricity data is measured at building level rather than system level, so only design data or document data can be selected in system or equipment level modeling. 2) Even if submeter data or BAs data is available, a universal calibration method and a standard calibration procedure are still lacking. Online real-time simulation is another area which requires even smaller time scale calibration with power data. So it has stringent demand on the computational speed of calibration algorithm [22]. However, matching the hourly power data with whole building power or submeters is unthinkable. For above reasons, it is important to develop standard and easy calibration procedures for a BESM for existing buildings with submetering system.

To solve the above problems, a new bottom-up calibration approach based on hourly electricity submetering data and HVAC cooling/heating loads is proposed in this paper. These data have become available in more large commercial buildings with centralized monitoring and control systems. For example, in California, all large commercial buildings have installed interval meters collecting electricity power consumption data every 15 min.

If data from electricity meters are used to calibrate models, the “non-unique solution” problems can be solved and calibrated models can be more accurate in reflecting building operation than they were before. Because electricity meters for key components measure consumption hourly, setting up a BESM through a bottom-up process can guarantee the accuracy of hourly simulation inputs such as lighting and equipment scheduling. This approach can be programmed and implemented automatically. The basic concept of the proposed calibration procedure is to separate non-HVAC calibration from HVAC-related calibration. Non-HVAC hourly energy

consumption inputs can be obtained by separating out non-seasonal patterns in the building power data. HVAC hourly energy consumption can be simulated accurately if the hourly cooling/heating load and HVAC equipment power consumption data are available. In this paper, the model calibration process and detailed methodology are presented in Section 3. A case study to demonstrate the procedure is illustrated in Section 4. In buildings where the cooling/heating load measurement is not available, a method is presented as well. However, its accuracy is a little worse than when load data are available.

2. Submeters and cooling/heating load measurement

Generally speaking, the total building energy consumption can be divided into four main submeters and several secondary submeters; see Fig. 1 [6,7]. A data measurement cycle of 5 min is good enough for model calibration. Submetering building energy consumption all of the way to the bottom is difficult. However, with a small budget, submetering to the second level from the top is easy. The average cost of submetering at this level in a 20,000-square-meter large commercial building is less than 10 K dollars. Many building control systems measure cooling/heating load by adding temperature sensors and flow meters on chilled water inlet and outlet pipes. Modern chillers have cooling load data and those data are retrievable with a manufacturer-provided communication card. However, it is important to note that cooling load data are less reliable then electric power data because of sensor drift.

The hourly energy consumption is calculated by following Eq. (1). As for cooling/heating load measurement, the acquired data are chilled water (hot water) inlet temperature, chilled water (hot water) outlet temperature and chilled water (hot water) flow rate; the cooling/heating load can then be calculated indirectly using Eq. (2).

$$E = \sum_{i=1}^{60/\tau} \left(P_i \times \frac{60}{\tau} \right) \tag{1}$$

$$\text{Hourly cooling/heating load} = \sum_{1}^{n} \left(\sum_{1}^{60/t} \left(CM_j \Delta T_j \times \frac{60}{t} \right) \right) \tag{2}$$

3. Model calibration methodology

The calibration method proposed in this paper is divided into six stages (see Fig. 2), among which stage 3 and stage 5 are the key parts. The data follow from top to bottom and HVAC-related data calibration is separated out from non-HVAC-related calibration in stage 3. The details of the six stages are demonstrated from Section 3.1 to 3.6. The parameters used in this calibration procedure are listed in Table 1.

3.1. Basic building information

This stage is no different from standard methods in construction BESMs. A complicated geometric model does not necessary lead to a more accurate BESM, but will slow down the model drastically. Depending on the purpose of the model, it is important to reasonably simplify building geometry and interior spaces. However, the degree of the simplification should be carefully checked since oversimplifying the zoning configuration in building simulations might result in large errors in cooling load calculations. Similar discussions can be referred to existing articles [25,38] and the details will not be discussed here.

3.2. Calibration of construction

Heat transfer through the building envelope (ground floor, external wall, external window and roof) is one of the main parts of a building's cooling/heating load. Building internal structures (internal floor and internal wall) and interior decoration (furniture, carpet, books and so on) do not affect the load by very much, but they have an impact on the lag in load change when indoor air temperatures are reset. After an on-site survey, the building envelope and main internal structures can be set up precisely in simulation tools, but it is difficult to simulate interior decoration accurately. Previous researchers, such as K.A. Antonopoulos and E. Koronaki [45], indicated that the heat storage capacity of the building envelope, main internal structures and interior decoration as percentages of the total capacity are 78%, 15% and 7%, respectively. Furthermore, Junli Zhou [46] concluded that in buildings with continuously operating HVAC systems, interior decoration temperatures and room temperatures are basically consistent; therefore, their impact on HVAC system load is almost negligible. Therefore, whether it is worth spending effort to accurately

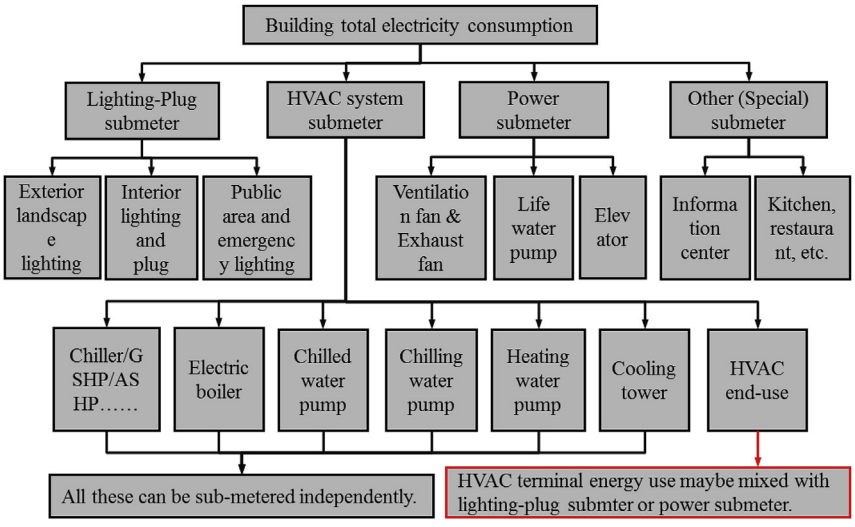

Fig. 1. Submetering structure.

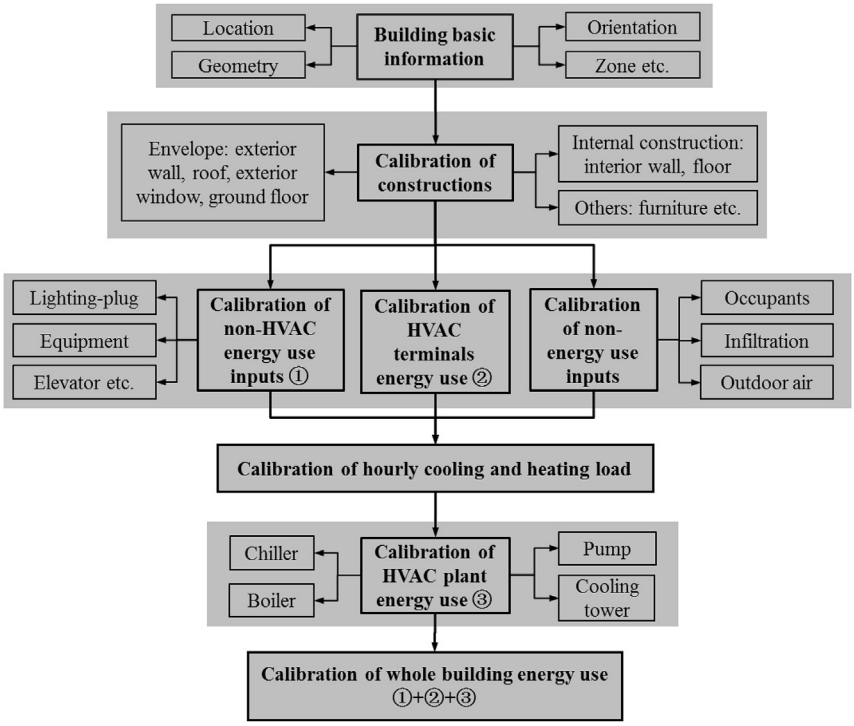

Fig. 2. Detailed calibration process of building energy simulation models.

simulate the internal structure depends on the purpose of the simulation models. If models are not used for demand response studies, the focus of this stage is on the building envelope and the main internal structures instead of the furnishings.

3.3. Calibration of non-HVAC energy use inputs, HVAC terminal energy use and internal non-energy use inputs

The calibrations of non-HVAC energy use inputs, energy use of HVAC terminals and internal non-energy use inputs are put together in this stage because, in many cases, these three parts are all related to internal heat gain.

Table 1
Parameters needed for the calibration method proposed in this paper.

Field		Input parameters
Construction	Envelope; Internal floor; Internal wall	Thickness of layers Conductivity of layers Density of layers Specific heat of layers
	External window	U-factor SHGC
Thermal zone	Energy use	Lighting power density Lighting schedule Equipment power density Equipment schedule
	Occupants	Occupant density Occupant schedule
	Outdoor air	Infiltration rate Outdoor air rate of HVAC system
HVAC system	Fans	Performance curve of fan Pressure rise Efficiency
	Pumps	Performance curve of pump Rated head Rated flow rate Rated power consumption Efficiency
	Cooling/Heating source	Performance curves of pump Reference capacity Reference COP

3.3.1. Calibration of non-HVAC energy use inputs

Previous studies [17–19] have proved that lighting and equipment energy use varies periodically, in daily and annual cycles. These non-HVAC energy uses are independent of ambient temperature and other weather variables in commercial buildings and can therefore be expressed by a Fourier series model, shown in Eqs. (3)–(3-4).

$$E_L(\text{or}E_P) = a + f(\mathrm{d}) + \varphi(\mathrm{h}) + \phi(\mathrm{d},\ \mathrm{h}) + \varepsilon \tag{3}$$

$$f(\mathrm{d}) = \sum_{m=1}^{m_{\max}} [\alpha_m \sin(2\pi\omega_\mathrm{m})\mathrm{d} + \beta_\mathrm{m}\cos(2\pi\omega_\mathrm{m})\mathrm{d}] \tag{3-1}$$

$$\varphi(\mathrm{h}) = \sum_{\mathrm{n}=1}^{\mathrm{n}_{\max}} [\delta_n \sin(2\pi\omega_\mathrm{n})\mathrm{h} + \eta_\mathrm{n}\cos(2\pi\omega_\mathrm{n})\mathrm{h}] \tag{3-2}$$

$$\phi(\mathrm{d},\ \mathrm{h}) = \sum_{m=1}^{m_{\max}} \sum_{\mathrm{n}=1}^{\mathrm{n}_{\max}} [\gamma_\mathrm{m} \sin(2\pi\omega_\mathrm{m})\mathrm{d} + \lambda_\mathrm{m}\cos(2\pi\omega_\mathrm{m})\mathrm{d}] \times [\mu_\mathrm{n} \sin(2\pi\omega_\mathrm{n})\mathrm{h} + \kappa_\mathrm{n}\cos(2\pi\omega_\mathrm{n})\mathrm{h}] \tag{3-3}$$

$$\omega_\mathrm{m} = \frac{\mathrm{m}}{365},\ \mathrm{m} = 1 \sim 182, \quad \omega_\mathrm{n} = \frac{\mathrm{n}}{24},\ \mathrm{n} = 1 \sim 12 \tag{3-4}$$

A further study [19] declared that for stable commercial buildings, variable “d” has almost no influence on the precision of the Fourier series model. So we ignore the variable “d” and simplify the model above to a simple format like that of Eq. (4). For example, shopping mall buildings generally have one day type, whereas office buildings have two types: “workday” and “non-workday” [19]. Different day types should be calculated separately.

$$E_L(\text{or}E_P) = a + \sum_{n=1}^{n_{max}}[\delta_n \sin(2\pi\omega_n)h + \eta_n\cos(2\pi\omega_n)h] + \varepsilon, \quad \omega_n = \frac{n}{24}, \quad n = 1 \sim 12 \tag{4}$$

Using the above Fourier series model, we can calculate the hourly submeter measurements in each day type. Specific Fourier series models to calculate hourly submeters are set up by using stepwise regression with full year cycle, and using hourly measured data as the training data. Stepwise regression includes regression models in which the choice of predictive variables is carried out by an automatic procedure. The computational software, such as Matlab, can be selected to iteratively adjust these parameters so that the predicted data match the measured data. Under the same day type, the maximum value of hourly energy consumption in each submeter is chosen as the set point, and the ratio of the value at other times to the maximum value is calculated as a fraction of the schedule. The proportions of convection and radiation heat from lamps and equipment are standard values from the ASHRAE Handbook [47].

3.3.2. Calibration of internal non-energy use inputs

Building internal non-energy use inputs mainly involve three parameters: occupants, air infiltration through the envelope, and outdoor air from HVAC systems.

In many office buildings, people need a chip card to enter and leave the building, even if just as a temporary visitor. Many modern shopping malls, Class-A office buildings, and hotels have visitor counting systems at the entrance and main traffic points. In this case, the occupant schedule is available for setting up the model. However, as for those buildings without occupant statistics, an on-site survey on typical days would be a feasible way of setting up the model. The ASHRAE Handbook has recommended values for the amount of sensible heat and latent heat per occupant, and the proportion of convection and radiation heat gain [47].

It is indeed difficult to measure or calculate the real-time air infiltration. However, some existing studies prove that the infiltration air rate is generally not more than 0.5 ac/h, and in air conditioning zones it is even smaller, at as little as 0.1 ac/h. Additionally, the cooling load of the air-conditioning system formed by infiltration air only accounts for 4% of the total cooling load [48–50]. Hence, according to the level of building air tightness and the position of the thermal zone, the air infiltration rate can be set between 0.1 and 0.5 ac/h. The outdoor fresh air rate at air handling units can be set according to the actual HVAC system situation.

3.3.3. Calibration of HVAC terminals energy use

It is very common that HVAC terminal electric circuits are mixed with lighting-plug circuits or power circuits. Therefore, it is necessary to expend some effort disaggregating mixed power data. As mentioned in Section 3.3.1, these non-HVAC energy uses are independent of ambient temperature and other weather variables in commercial buildings and can therefore be expressed by a Fourier series model. Generally speaking, HVAC system is turned off in transition seasons, so the lighting-plug and power submeter data in transition seasons is unmixed. Thus, the hourly lighting-plug and power submeter data can be regressed by Eq. (4) with transition seasons' data and the trained models can be used to calculated hourly lighting-plug and power submeters in heating and cooling seasons. Next, HVAC terminal energy consumption is obtained by subtracting the calculated lighting-plug or power submeter data from the mixed data which is measured directly [19]. If the HVAC terminal units are measured independently, the calibration can be carried out directly. The detailed calibration process for HVAC terminals is clarified in Section 3.5.

3.4. Calibration of hourly cooling and heating load

Modern BESMs are relatively accurate in simulating building cooling/heating load if the inputs are correct. Thus, the key task in this stage is to compare the simulated load with the actual load calculated by Eq. (2), and then adjust the BESM inputs according to the analysis results. Because the simulation of the building envelope and internal energy use are relatively accurate, the adjustment focuses on occupants and air infiltration from the initial values above. No adjustment to the HVAC system is needed here.

In this stage one important step is the setting of indoor air temperature and relative humidity. The indoor air temperature and absolute humidity is determined in Eqs. (5-1) and (5-2) respectively as the weighted average of the temperature or absolute humidity at different spatial locations. The return air temperature of a HVAC terminal or the measured temperature in a zone both can be used as T_i. And the absolute humidity can be translated to relative humidity easily. After the running of models, the comparison of temperature and relative humidity set points and model output data should be conducted.

$$\overline{T} = \frac{\sum T_i V_i}{\sum V_i} \tag{5-1}$$

$$\overline{H} = \frac{\sum H_i V_i}{\sum V_i} \tag{5-2}$$

3.5. Calibration of HVAC plant energy use

The main energy consumption components of an HVAC system are chillers, heat sources (heat pumps or boilers), pumps (chilled pumps, chilling pumps and hot water pumps), and fans (terminal fans and cooling tower fans). These main components must be calibrated one by one. In this paper, gas and oil heating sources are not addressed because buildings do not normally have hourly gas consumption data. Only power submeters are used in the calibration process.

Chiller. In many existing simulation tools, two or more curves must be set correctly for the chiller. Taking EnergyPlus as an example, three curves are needed: 1) a Cooling Capacity as a Function of Temperature Curve (ChillerCapFTemp), 2) an Energy Input to Cooling Output Ratio as a Function of Temperature Curve (ChillerEIRFTemp) and 3) an Energy Input to Cooling Output Ratio as a Function of the Part Load Ratio Curve (reciprocal of COP (coefficient of performance)). Calibration of the COP curve is the most important (Eq. (6-3)), and the other curves (Eqs. (6-1) and (6-2)) can be fixed with defaults or examples from EnergyPlus models, if there is no sufficient training data. This point is further demonstrated in the case study later. The format of the COP curve is described by Eq. (6-3).

$$ChillerCapFTemp = m_0 + m_1(T_{el}) + m_2(T_{el})^2 + m_3(T_{ce}) + m_4(T_{ce})^2 + m_5(T_{el})(T_{ce}) \tag{6-1}$$

$$ChillerEIRFTemp = n_0 + n_1(T_{el}) + n_2(T_{el})^2 + n_3(T_{ce}) + n_4(T_{ce})^2 + n_5(T_{el})(T_{ce}) \tag{6-2}$$

$$COP = c_0 + c_1(PLR) + c_2(PLR)^2 + c_3(PLR)^3 \quad (6\text{-}3)$$

Heat source. If the heat source is a heat pump, the calibration method is same as for the chiller. If it is an electric boiler, the actual boiler efficiency can be calculated using heating load, energy use and other parameters from the catalog.

Pumps. The pump performance curve is regressed with the actual pump energy consumption and the flow rate as a function of the partial load factor, as in Eq. (7). Fractions (8-1) and (8-2) are useful if the water flow rate is unavailable.

$$P_{pl} = p_0 + p_1(PPLR) + p_2(PPLR)^2 + p_3(PPLR)^3 \quad (7)$$

$$P_{pump} = P_{pl} \times P_{design} \quad (8)$$

$$\text{Chilled pump}: \quad PPLR = \frac{Q_{actual}}{C\rho\Delta T_{actual}F_{design}} \quad (8\text{-}1)$$

$$\text{Chilling pump}: \quad PPLR = \frac{Q_{actual} + P_{chiller}}{C\rho\Delta T'_{actual}F'_{design}} \quad (8\text{-}2)$$

Fans. In some cases, the hourly electricity consumption of terminal fans and cooling tower fans is directly measured in the submetering system. In other cases, the data for terminal fans can be calculated using the process introduced in Section 3.3. This is true if the air flow rate is also available. The fan performance curve can be fitted using a model (Eq. (9)). If the air flow rate is unavailable, which is true in most cases, indirect calculations can be made using Eqs. (10-1)–(10-5). The energy use of terminal fans calculated here is the total energy consumption of all terminals. The performance curve is an equivalent total performance curve.

$$F_{pl} = f_0 + f_1(FPLR) + f_2(FPLR)^2 + f_3(FPLR)^3 \quad (9)$$

$$P_{fan} = F_{pl} \times F_{design} \quad (10)$$

$$\text{Terminal unit fans}: \quad FPLR = \frac{Q_{actual}}{C'\rho'\Delta T_{air}F_{airdesign}} \quad (10\text{-}1)$$

$$\text{Closed cooling tower}: \quad FPLR = \frac{CM\Delta T'_{actual}}{C'\rho'\Delta T'_{air}F'_{airdesign}}; \quad (10\text{-}2)$$

$$FPLR = \frac{Q_{actual} + P_{chiller}}{C'\rho'\Delta T'_{air}F'_{airdesign}} \quad (10\text{-}3)$$

$$\text{Open cooling tower}: \quad FPLR = \frac{CM\Delta T'_{actual}}{\rho'\Delta H_{air}F'_{air\ design}}; \quad (10\text{-}4)$$

$$FPLR = \frac{Q_{actual} + P_{chiller}}{\rho'\Delta H_{air}F'_{airdesign}} \quad (10\text{-}5)$$

The calibration methods for pumps and fans studied in this article are suitable for variable speed types. As for single-speed or two-speed devices, the rated parameters are good enough for calibration.

3.6. Calibration of whole-building energy use

After non-HVAC energy consumption and the performance curves of the main HVAC equipment have been successfully calibrated, the next step is whole-building simulation. Some criteria are selected to evaluate the model and the definitions, as shown in Eqs. (11) and (12).

$$\text{Coefficient of variability (CV)} \quad CV = \frac{\sqrt{\left(\sum_{i=1}^{N}(E_{Mi} - E_{Pi})^2\right)/N}}{\left(\sum_{i=1}^{N}E_{Mi}\right)/N} \quad (11)$$

$$\text{Mean relative error (MRE)} \quad MRE = \frac{\sum_{i=1}^{N}|E_{Mi} - E_{Pi}|}{\sum_{i=1}^{N}E_{Mi}} \quad (12)$$

4. Case study

4.1. Building description

The target building, called “A,” is located in the Shanghai urban area. It is a multi-purpose commercial building with shopping malls and offices. There are eight floors, from the second floor underground (B2) to the sixth floor above the ground (F6). The second floor underground is non-air-conditioned space and used as the HVAC plant and facility rooms. From the first floor underground to the fourth floor is a shopping mall. The fifth and sixth floors are office zones. The total building area of building A is approximately 68,000 m^2 and the story height is 4.5 m. Building A covers an area of 9112 m^2 in an irregular shape with a length of 153 m and a width of between 51 m and 75 m. The window-to-wall ratio of each side is 18% (east), 40% (south), 18% (west) and 10% (north). The plan and outline drawings are shown in Fig. 3. A summarized list of power submeters is presented in Table 2.

The main HVAC equipment for this building is located on the second floor underground. The cooling tower is on the roof and AHUs (Air Handling Units) are on each floor they service. The equipment details are listed in Table 3. Based on the on-site survey, the cooling period is from May 1st to Oct. 30th and the heating period is from Dec. 1st to Mar. 1st. The indoor air temperature set point is 26 °C in summer and 18 °C in winter.

Building A is a multi-purpose commercial building; therefore, its model calibration is more difficult than that of a single-function building. A successful BESM calibration for this building, using the procedures we proposed, can demonstrate that BESM calibration works for both office buildings and other commercial buildings. The cooling load in this building is collected for a period from Aug. 12th to Sep. 30th at 5-min intervals.

4.2. Model calibration

4.2.1. Basic building information

Keeping the building area unchanged, the geometrical shape is simplified to a rectangle (152 m × 60 m) in the simulation environment, and the height is the same as that of the real building. In the real building, there are four AHUs on each floor; therefore, each floor of the model is divided into four zones. To obtain real-time weather data, a small weather station was built and the data acquisition began in Apr. 2014. The recording cycle is 10 min and the average value is used as the hourly value. The collected data includes outdoor air dry-bulb temperature, relative humidity, horizontal solar radiation and wind speed and direction. The

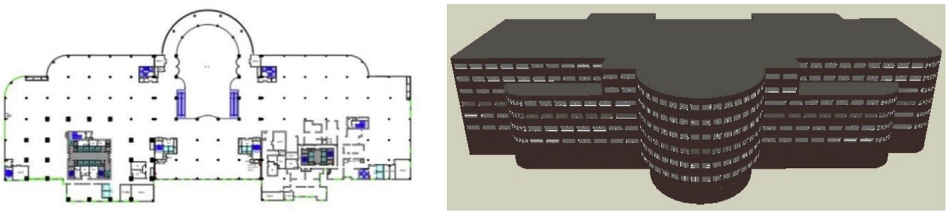

(a) (b)

Fig. 3. The plan drawing (a) and outline drawing (b) of the building analyzed in this paper.

Table 2
Submeters summary of building A.

Main submters	Directly measured	Secondary submeters	Directly measured	Source of building cooling/heating load
Lighting-plug submeter	Yes	Lighting and plug	No	Yes
		Exterior landscape lighting	Yes	No
		Corridor and public area lighting	No	Yes
Power submeter	Yes	Elevator	Yes	No (motor is on the roof)
		Non-HVAC water pump	No	Yes
		Ventilation/Exhaust fan	No	Yes
HVAC submeter	No	Terminal units	Yes	Yes
		Chiller	Yes	No (located in non-air-conditioning space)
		Chilled pump	Yes	
		Chilling pump	Yes	
		Cooling tower	Yes	
		Heat source	Use gas	
		Hot water pump	No	
Others/Specials	Yes	Information center	Yes	Independent air-conditioning

outdoor air dry-bulb temperature, relative humidity and horizontal solar radiation are the most important and are shown in Fig. 4.

4.2.2. Building calibration

The material layers of the building envelope and main internal structures are summarized in Table 4. As stated in Section 3.2, interior decoration has a small effect when simulating the building cooling/heating load in buildings with continuous HVAC systems; the decoration setting in this case is simply an estimated value.

4.2.3. Calibration of non-HVAC energy use inputs, HVAC terminal energy use and internal non-energy use inputs

4.2.3.1. Calibration of non-HVAC energy use inputs. According to Table 2, there are five non-HVAC submeters: 1) information center, 2) exterior landscape lighting, 3) lighting-plug submeter (excluding exterior landscape lighting), 4) elevator and 5) power submeter (excluding elevator).

Analysis of the historical submetering data showed that the information center runs all day throughout the year and the open time for the exterior landscape lighting is 18:00–24:00 throughout the year. As shown in Fig. 5, the hourly energy consumption of the information center fluctuates approximately 50 kWh and the

Table 3
Detailed descriptions of the equipment of HVAC system in building A.

Cold source	Number	Cooling capacity (kW)	Power (kW)	Chilled water flow rate (m^3/h)	Chilling water flow rate (m^3/h)
York centrifugal chiller	2	3516	591	605	706

Heat source	Number	Heating capacity (kW)	Power (kW)
LiBr absorption unit	2	2813	591

Pumps	Number	Flow rate (m^3/h)	Head (m)	Power (kW)	Type
Chilled pump	3 (one backup)	600	35	75	Variable speed
Chilling pump	3 (one backup)	720	32	90	Fixed speed
Hot water pump	3 (one backup)	120	30.5	15	Fixed speed

Cooling device	Number	Power (kW)	Water flow rate (m^3/h)	Fan diameter (mm)	Air flow rate (m^3/h)	Type
Cooling tower	4	5.5	175	2400	94,300	Two speed

Terminals	Number	Air flow rate (m^3/h)	Cooling capacity (kW)	Max power (kW)	Location	Head (Pa)
AHU	4 × 1	26,000	215	18.5	B1	200–800
AHU	2 × 4	32,000	257	18.5	F1–F4	200–800
AHU	2 × 4	36,000	283	22	F1–F4	200–800
AHU	2 × 2	21,000	174	15	F5–F6	200–800
AHU	2 × 2	32,000	257	18.5	F5–F6	200–800

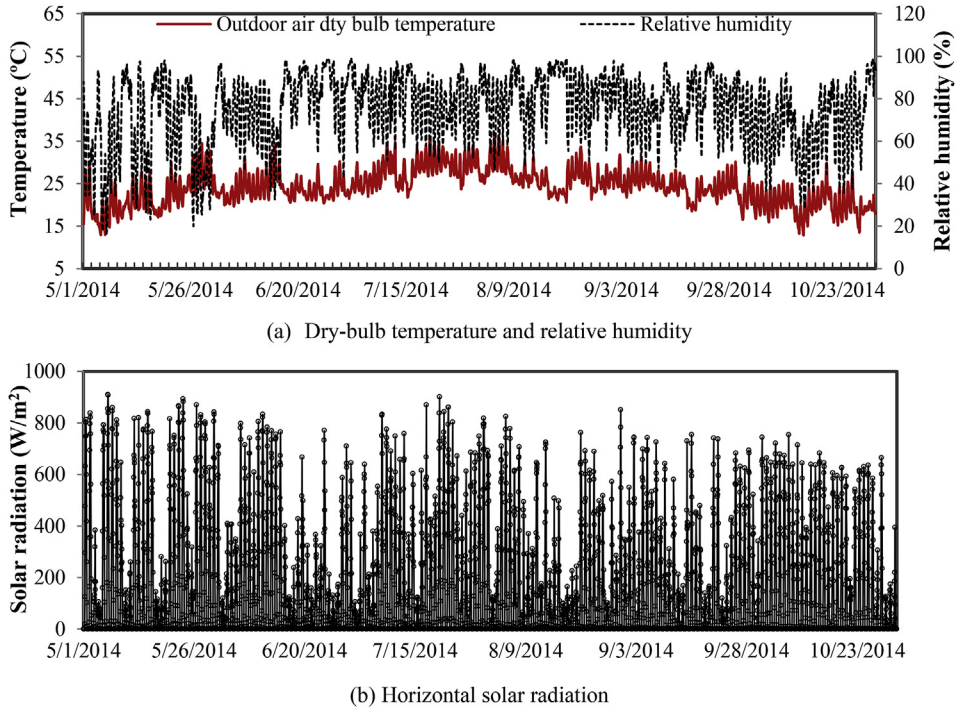

Fig. 4. The weather data of Shanghai from May 2014 to Oct. 2014.

maximum fluctuation is not larger than 3 kWh. Thus, the power usage for the information center is set at a constant 50 kW in the model. Similarly, the hourly energy consumption of the exterior landscape lighting fluctuates approximately 55 kWh and the maximum deviation is only 5 kWh. Thus, the power usage of exterior landscape lighting is set at a constant 55 kW in the model.

Swing seasons' submeter data are used to train and validate the Fourier series model described in Section 3.3.1, Eq. (4). The training data for spring (from Mar. 29th 2014 to Apr. 27th 2014) and validation data for fall (from Nov. 1st, 2014, to Nov. 30th, 2014) are illustrated in Fig. 6. As described in the "day type" concept [19], a power submeter (excluding the elevator) has only one day type.

Table 4
Material layers of building envelope and main internal structures.

	Layers	Thickness (mm)	Conductivity (W/m °C)	Density (kg/m^3)	Specific heat (J/kg °C)
Envelope					
Roof	Insulation mortar	20	0.08	400	1045.8
	Expanded perlite	50	0.16	400	1170
	Reinforced concrete	200	1.74	2500	920
	Cement mortar screeding	30	0.93	1800	1050
	Lime mortar	20	0.81	1600	1050
External wall	Granite	20	3.49	2800	920
	Insulation mortar	20	0.08	400	1045.8
	Cement mortar screeding	30	0.93	1800	1050
	Concrete block	200	0.68	1300	537.8
	Lime mortar	30	0.81	1600	1050
External window	Ordinary glass	3			
	Air space	6			
	Ordinary glass	3			
Ground floor	Cement base insulation mortar	300	0.085	450	1164.8
	Reinforced concrete	500	1.74	2500	920
	Cement mortar screeding	30	0.93	1800	1050
Internal structures					
Internal floor	Lime mortar	30	0.81	1600	1050
	Insulation mortar	20	0.08	400	1045.8
	Reinforced concrete	120	1.74	2500	920
	Lime mortar	30	0.81	1600	1050
Internal wall	Lime mortar	30	0.81	1600	1050
	Reinforced concrete	120	1.74	2500	920
	Lime mortar	30	0.81	1600	1050
Decoration 1	Wood 1	10	0.29	500	2510
Decoration 2	Wood 2	20	0.23	600	1890
Decoration 3	Fiberboard	50	0.29	500	2510

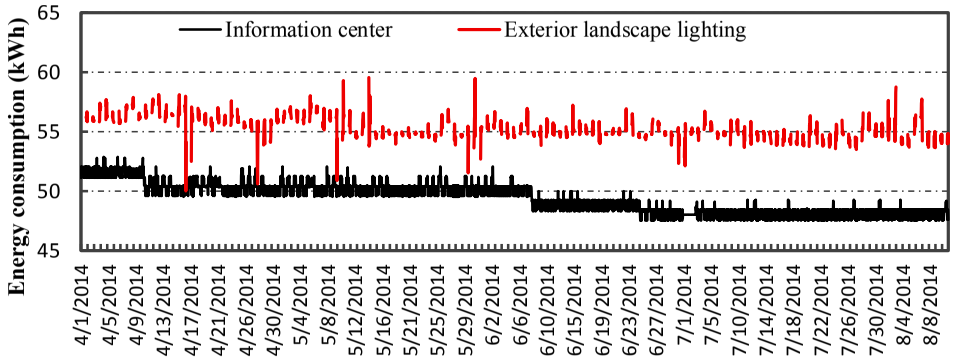

Fig. 5. Hourly electricity consumption of information center and exterior landscape lighting.

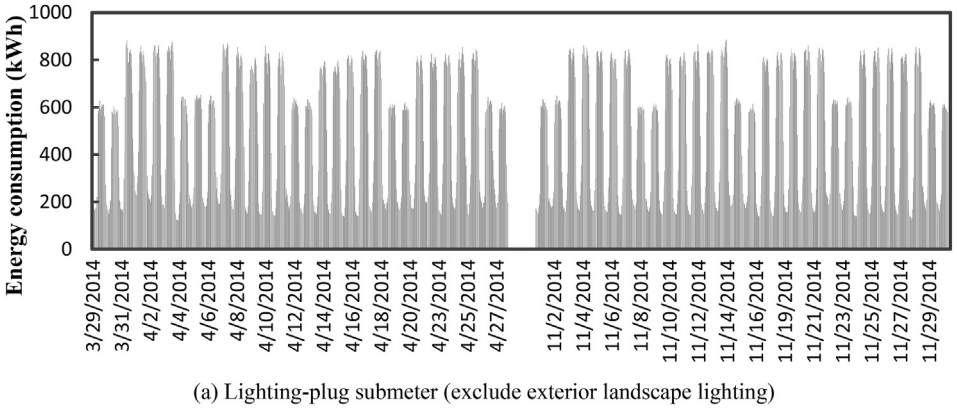

(a) Lighting-plug submeter (exclude exterior landscape lighting)

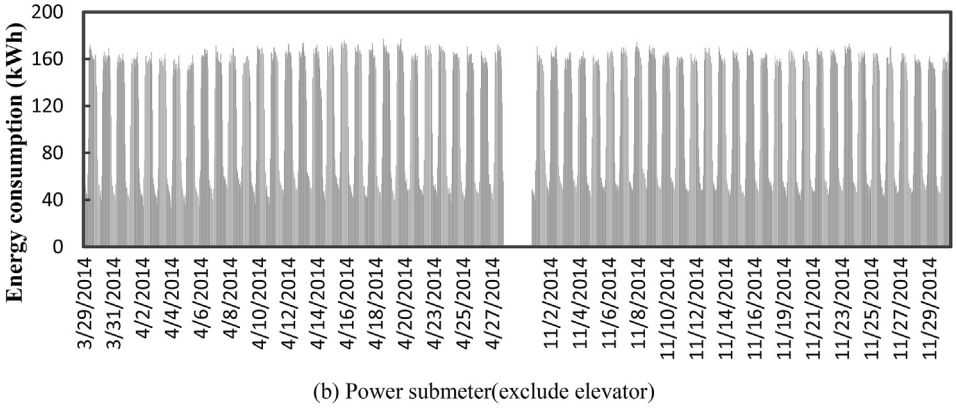

(b) Power submeter(exclude elevator)

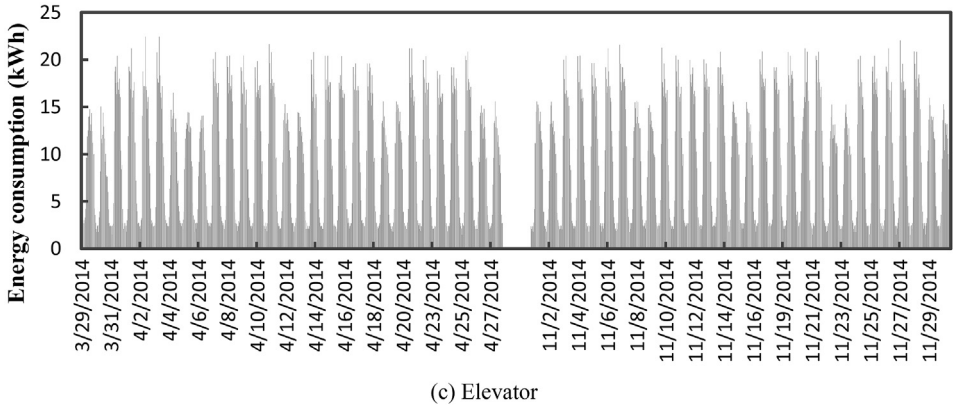

(c) Elevator

Fig. 6. Submeters selected to training and validating Fourier series models.

Table 5
Fitted parameters of each Fourier series model.

Parameter	Lighting-plug submeter (exclude exterior landscape lighting)		Power submeter(exclude elevator)	Elevator	
	Workday	Non-workday	Full year	Workday	Non-workday
a	538.9	418.4	115	10.29	8.102
δ_1	−331.2	−239.2	−62.78	−5.99	−4.75
δ_2	−64.58	−25.66	−10.2	−0.5207	−0.2729
δ_3	−5.099	−9.168	0.02581	1.503	0.3642
δ_4	−25.04	−20.51	−9.781	−0.6794	−0.253
δ_5	9.065	17.1	3.968	0.1522	0.09128
δ_6	−9.292	−11.35	−1.793	−0.3013	0.142
δ_7	10.88	16.38	0.8318	−0.01698	0.1782
δ_8	2.618	3.365	0.9028	0.3804	0.2001
δ_9	−0.7763	−0.2718	−0.455	0.2404	−0.007062
δ_{10}	8.833	10.23	1.759	−0.07978	0.07178
δ_{11}	−2.803	−2.431	−0.5772	0.1001	0.1251
δ_{12}	0.008974	0.3846	0.2978	0.4185	0.1344
η_1	−172.7	−109.9	−29.86	−6.828	−4.303
η_2	50.25	32.85	11.6	1.104	0.7342
η_3	−78.74	−62.53	−14.97	−1.175	−0.9785
η_4	−3.568	−5.959	−2.573	−0.3972	−0.2099
η_5	−12.31	−16.59	−2.195	1.149	0.03713
η_6	−16.96	−19.04	−4.719	−1.177	−0.3673
η_7	4.573	5.321	0.51	0.156	−0.1053
η_8	−12.95	−10.92	−2.206	−0.3059	0.1524
η_9	4.223	1.814	0.2883	0.01949	−0.06603
η_{10}	−0.3947	1.21	−0.6294	0.3908	0.002889
η_{11}	0.5534	−1.459	−1.161	−0.2924	0.3023
η_{12}	1.446	2.761	1.008	0.2444	−0.04701

Table 6
Results of training model and validating model of each submeters analyzed in this study.

Submeter	Day type	Training model R^2	Training model CV (%)	Training model MRE (%)	Validating model CV (%)	Validating model MRE (%)
Lighting-plug submeter (exclude exterior landscape lighting)	Workday	0.9850	6.529	4.772	4.518	4.255
	Non-workday	0.9836	6.357	4.433	3.074	3.825
Elevator	Workday	0.9886	7.271	5.181	8.561	6.596
	Non-workday	0.9542	13.23	8.838	6.709	8.508
Power submeter (exclude elevator)	Full year	0.9745	7.479	4.685	5.482	4.082
Total non-HVAC energy use	–	–	–	–	3.980	2.921

Table 7
Schedules set in building energy simulation model of this case building.

Submeters		Lighting-plug submeter					Power submeter			Others
		Lighting-plug submeter of office area in workdays	Lighting-plug submeter of shopping area	Night lighting in workdays	Night lighting in non-workdays	Exterior landscape lighting	Elevator in workdays	Elevator in non-workdays	Power submeter (excluding elevator)	Information center
Peak value (Kw)		227	628	303		55	21		166	50
Area (m^2)		18,000	45,000	63,000	63,000				63,000	
Density (W)		12.61	13.96	4.81	4.81				2.63	
Schedule	1:00	0.00	0.00	0.63	0.66	0.00	0.12	0.12	0.33	1.00
	2:00	0.00	0.00	0.58	0.63	0.00	0.11	0.11	0.31	1.00
	3:00	0.00	0.00	0.56	0.58	0.00	0.11	0.11	0.29	1.00
	4:00	0.00	0.00	0.54	0.54	0.00	0.11	0.11	0.28	1.00
	5:00	0.00	0.00	0.54	0.54	0.00	0.11	0.11	0.27	1.00
	6:00	0.00	0.00	0.68	0.60	0.00	0.13	0.14	0.25	1.00
	7:00	0.35	0.32	0.00	0.00	0.00	0.23	0.20	0.33	1.00
	8:00	0.63	0.37	0.00	0.00	0.00	0.57	0.40	0.48	1.00
	9:00	0.77	0.76	0.00	0.00	0.00	0.94	0.51	0.87	1.00
	10:00	0.89	0.95	0.00	0.00	0.00	0.87	0.62	1.00	1.00
	11:00	0.92	0.96	0.00	0.00	0.00	0.82	0.64	0.99	1.00
	12:00	1.00	0.96	0.00	0.00	0.00	0.80	0.68	0.98	1.00
	13:00	0.82	1.00	0.00	0.00	0.00	0.98	0.65	0.98	1.00
	14:00	0.72	0.99	0.00	0.00	0.00	0.83	0.67	0.99	1.00
	15:00	0.78	0.94	0.00	0.00	0.00	0.79	0.60	1.00	1.00
	16:00	0.83	0.97	0.00	0.00	0.00	0.75	0.59	0.99	1.00
	17:00	0.88	0.98	0.00	0.00	0.00	0.80	0.62	0.99	1.00
	18:00	0.96	0.97	0.00	0.00	1.00	0.80	0.55	0.98	1.00
	19:00	0.90	0.97	0.00	0.00	1.00	0.58	0.50	0.99	1.00
	20:00	0.78	0.96	0.00	0.00	1.00	0.43	0.45	0.98	1.00
	21:00	0.65	0.89	0.00	0.00	1.00	0.41	0.39	0.91	1.00
	22:00	0.54	0.57	0.00	0.00	1.00	0.23	0.20	0.67	1.00
	23:00	0.00	0.00	1.00	0.78	1.00	0.15	0.15	0.42	1.00
	0:00	0.00	0.00	0.75	0.72	1.00	0.13	0.14	0.36	1.00

Lighting-plug submeters (excluding exterior landscape lighting) and elevators have two day types: “workday” and “non-workday”.

The parameter training result for each model is listed in Table 5 and the training and validation analysis is shown in Table 6. All R^2 values for the training models are larger than 0.95. The best result is for the lighting-plug submeter (excluding exterior landscape lighting) on non-workdays, with a CV (coefficient of variation) of 3.074% and MRE (mean relative error) of 3.825%. The worst is the elevator on non-workdays, though the CV (6.709%) and MRE (8.508%) are still controlled within 10%. The simulation result for total non-HVAC energy is excellent. The CV is 3.980% and MRE is 2.921%. The result is acceptable.

After this step, the hourly electricity consumption and maximum value of each submeter are determined and setting the model becomes very simple. The design value is chosen as the maximum electricity consumption for each submeter, and the ratio of the value at any other hour to the maximum is calculated as the schedule. With this method, the schedules in this case are listed in Table 7. The lighting and plug are mixed together, but it is not necessary to separate them out because they are treated similarly in

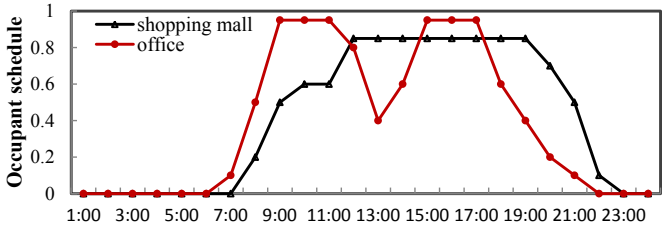

Fig. 8. Occupant schedule of this case.

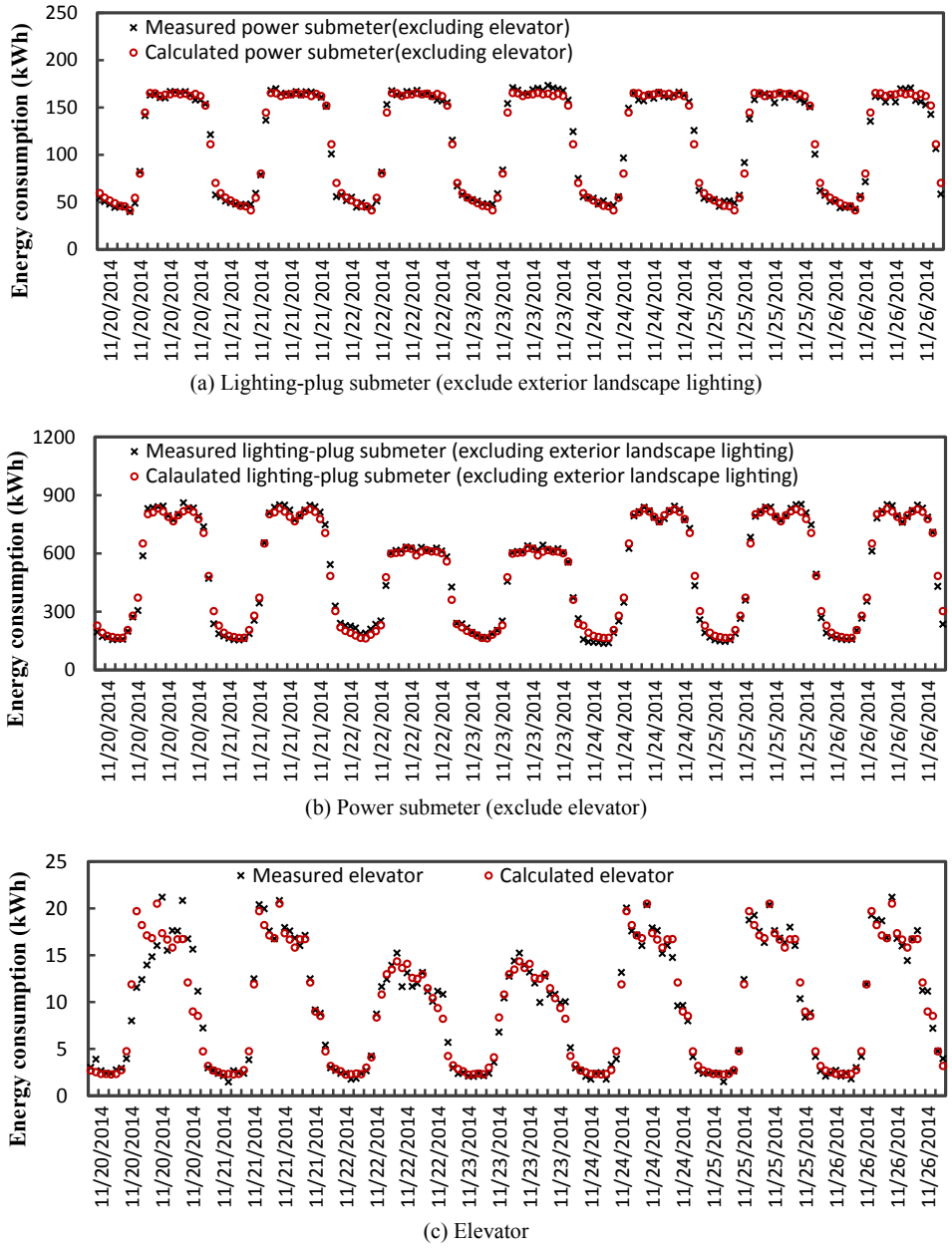

Fig. 7. Comparison of measured submeters and simulated submeters for one week.

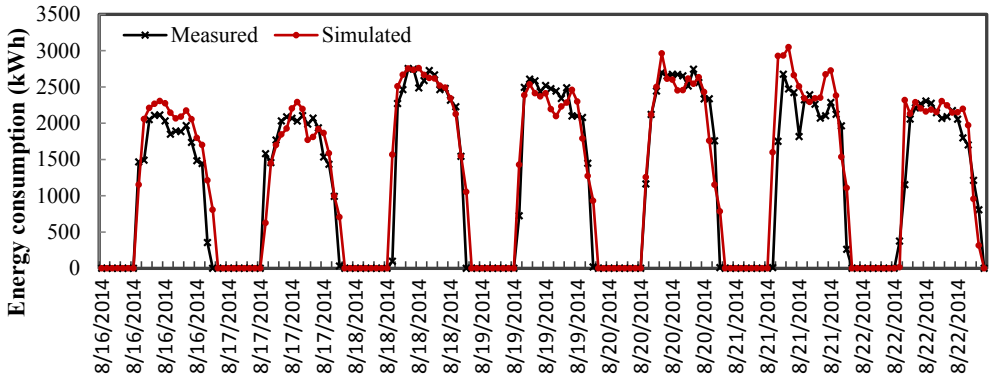

Fig. 9. Comparison of the simulated load and the actual load.

internal load calculations. To illustrate the simulation results, a one-week comparison of measured submeters and simulated submeters is shown in Fig. 7.

4.2.3.2. Calibration of internal non-energy use inputs. There is no system for occupant statistics in building A. An on-site survey concluded that the peak occupant density of the office area is 8 m^2/person on workdays and that of the shopping area is 6 m^2/person. The schedules are shown in Fig. 8. Latent heat, convective heat and radiant heat contribute 40%, 20% and 40% of occupancy heat gains, respectively [47].

According to the study in Section 3.3.2, the air infiltration rate is set between 0.1 and 0.5 ac/h. The shape coefficient and window-to-wall ratio of this building are both relatively small. This means the air infiltration rate is not too large. Thus, 0.1 ac/h is used in this model.

It is recommended to set the outdoor air rate based on the actual conditions of the HVAC system. In this particular HVAC system, one AHU serves as a fresh air unit on each floor and has a fixed outdoor air rate of approximately 1 ac/h; therefore, the outdoor air rate in this model is also set to 1 ac/h.

4.2.3.3. Calibration of HVAC terminal energy use. In accordance with the information listed in Table 2, the HVAC terminal units are directly metered. Therefore, there is no need for a disaggregation step. The process and results of HVAC terminal unit calibration are explained in detail in Section 4.2.5.

4.2.4. Calibration of hourly cooling and heating load

At this point, all parts with influence on simulating building cooling and heating loads have been completely calibrated. The task at this step is to compare and analyze the simulated cooling load and measured cooling load. One week of data from Aug. 16th, 2014, to Aug. 22nd, 2014, is extracted and illustrated in Fig. 9. The result is acceptable, with a CV of 13.40% and an MRE of 8.242%. The elevator and outdoor landscape lighting have nothing to do with the HVAC cooling load because the released heat is outside of the building. The information center has its own dedicated air conditioning system; therefore, it is also not included in the central HVAC system load.

4.2.5. Calibration of HVAC plant energy use

The main equipment simulations are calibrated one by one, following these three steps: Step 1, fit the performance curve of each piece of equipment; Step 2, set the curves in the simulation tools; and Step 3, compare the simulated result with the measured data.

Submetering data and cooling load measurement data are available in this building; therefore, the energy consumption data for each chiller and pump, hourly cooling load and chilled water flow rate are available. The COP curve for a Chiller and performance curve for a pump are fitted by Eqs. (6-3) and (7). The results are given in Table 8. Terminal fans have no air flow rate meters, but the room air temperature and HVAC-supplied air temperature are known to be 26 °C and 18 °C. Thus, the FPLR can be calculated using Eq. (10-1). The result is also summarized in Table 8.

As is shown in Fig. 10, the performance curve for a single pump and the equivalent performance curve for the terminal fans fit cleanly and tightly with measured data. However, the COP-measured points are more scattered. In many simulation tools, the COP is not a single variable function of PLR; it is correlated with chilled water inlet/outlet temperatures and chilling water leaving/entering temperatures. In this study Eq. (6-1) and (6-2) are fixed with defaults in EnergyPlus, because there is no sufficient training data. Even so, the simulated COP and the calculated COP still match very well.

4.2.6. Calibration of whole building energy use

The last step is to summarize the entire model calibration process discussed up to this point. Through the calibration, every submeter of non-HVAC energy use is simulated and the maximum mean deviation is still within 10%. The non-HVAC electricity consumption simulation is very good. The hourly CV and MRE are only 3.980% and 2.921% (see Table 6). The HVAC system calibration result is also satisfactory, and the details are listed in Table 8. As for the building cooling load simulation, a CV of 13.40% and MRE of 8.242% are not as good as other values, but are still acceptable. There are

Table 8
Summary of HVAC plant calibration results.

Model	R^2	CV (%)	MRE (%)
$COP = 1.913 + 12.14(PLR) - 7.557(PLR)^2$	0.7235	11.50	9.380
$P_{pl} = 0.6024 - 0.8161(PPLR) + 2.883(PPLR)^2 - 1.720(PPLR)^3$	0.8845	5.306	4.249
$F_{pl} = 0.3244 + 1.324(FPLR) - 1.052(FPLR)^2 + 0.3384(FPLR)^3$	0.8673	4.873	3.733

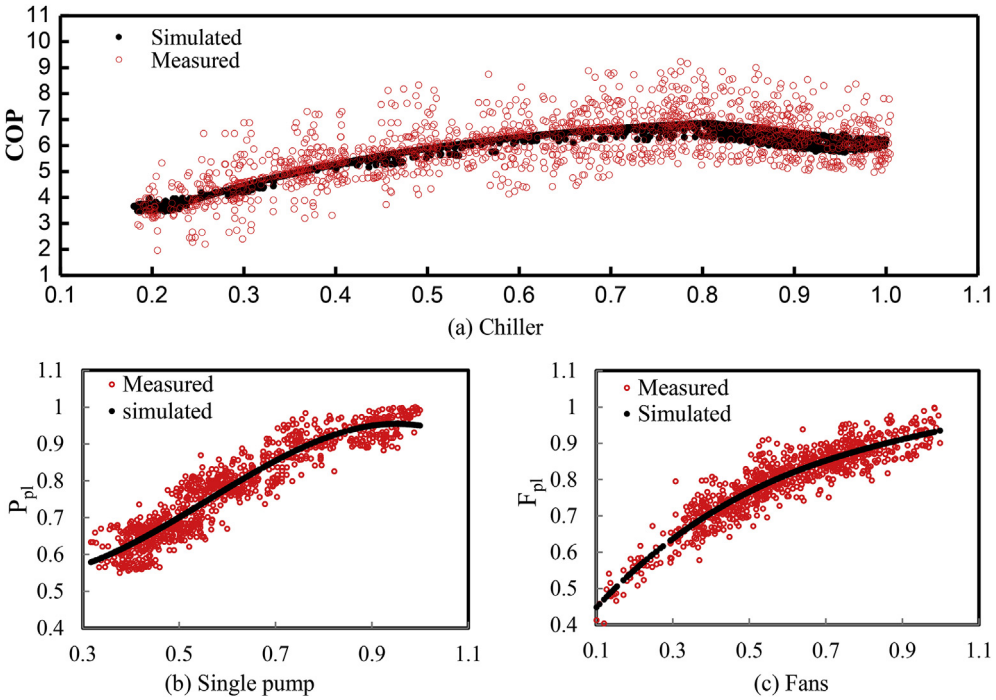

Fig. 10. Calibration results of HVAC main devices.

several factors resulting in the inaccuracy of the cooling load: 1) Although the building envelope and main internal structures are set according to the actual material layers, some parts of the building envelope are not built as designed; 2) There are still some differences between the occupant settings and actual conditions; and 3) The air infiltration rate and HVAC outdoor air rate may change from time to time and are not fixed values.

5. Conclusions and future work

Calibrating the BESM for an existing building is difficult, and there are no standard procedures. A new, bottom-up calibration approach based on hourly electricity submetering data and HVAC cooling/heating load is proposed, and a six-step calibration process is presented in this paper. A detailed case study is described to illustrate the procedure. The key new development in this new BESM calibration process is the use of a Fourier series model to estimate hourly non-HVAC electricity consumption from power meters. The case study demonstrated that the calibration of each non-HVAC submeter can be performed very accurately, with a maximum CV and MRE of only 8.651% and 8.508%, respectively (see Table 6). The result of the HVAC system and cooling load calibration is also satisfactory (see Table 8).

Although the case study demonstrated that this calibration method is applicable and the procedure is more efficient than conventional ways of comparing monthly electricity bills, the proposed method still has some shortcomings and deficiencies. In this case study, all calibrations are completed manually. This not only requires skilled engineers with professional knowledge but also costs much time. To expand the application and improve its efficiency, future studies should use automatic calibrations following the same procedures.

References

[1] Wang Qingyi. Building energy consumption statistics and computing research in China. Energy Conserv Environ Prot 2007;8:9–10.
[2] Key World Energy Statistics, 2009, IEA.
[3] DOE. Buildings energy data book, office of energy efficiency and renewable energy. US Department of Energy, 2011. 2010.
[4] Council, E.P.A. Directive 2010/31/EU of the European Parliament and of the Council of 19 May, 2010 on the energy performance of buildings. Off J Eur Union 2010:13–35.
[5] Annual Report on China Building Energy Efficiency Building energy conservation research center of Tsinghua University. 2013. http://www.amazon.cn/dp/B00C387HXA [In Chinese].
[6] Akbari H. Validation of an algorithm to disaggregate whole-building hourly electrical load into end uses. Energy 1995;20:1291–301.
[7] Ghiaus C. Experimental estimation of building energy performance by robust regression. Energy Build 2006;38(6):582–7.
[8] Manfren Massimiliano, Aste Niccolò, Moshksar Reza. Calibration and uncertainty analysis for computer models – a meta-model based approach for integrated building energy simulation. Appl Energy 2013;103:627–41.
[9] Azadeh A, Ghaderi SF, Sohrabkhani S. Annual electricity consumption forecasting by neural network in high energy consuming industrial sectors. Energy Convers Manag 2008;49(8):2272–8.
[10] Ekici Betul Bektas, Aksoy U Teoman. Prediction of building energy consumption by using artificial neural networks. Adv Eng Softw 2009;40:356–62.
[11] Magnier L, Haghighat F. Multiobjective optimization of building design using genetic algorithm and artificial neural network. Build Environ 2010;45:739–46.
[12] Bo-Juen Chang Ming-Wei, Lin C-J. Load forecasting using support vector machine: a study on EUNITE competition 2001. IEEE Trans Syst 2004;19(4):1821–30.
[13] Dong B, Cao C, Lee SE. Applying support vector machines to predict building energy consumption in tropical region. Energy Build 2005;37(5):545–53.
[14] Qiong Li, Qinglin Meng, Jiejin Cai, Hiroshi Yoshino, Akashi Mochida. Applying support vector machine to predict hourly cooling load in the building. Appl Energy 2009;86(10):2249–56.
[15] Wehenkel L, Pavella M. Decision tree approach to power systems security assessment. Int J Electr Power Energy Syst 1993;15(1):13–36.
[16] Yu Zhun, Haghighat Fariborz, Fung Benjamin CM, Yoshino Hiroshi. A decision tree method for building energy demand modeling. Energy Build 2010;42:1637–46.
[17] Dhar A, Reddy TA, Claridge D. A fourier series approach to predict hourly heating and cooling energy use in commercial buildings with outdoor temperature as the only weather variable. In: ASME/JSME/JSES International solar energy Conference, Mawuii, Mar. 27-30, vol. 1; 1995. p. 125–34. Accepted for publication in ASME Journal of Solar Energy Engineering.
[18] Dhar A, Reddy TA, Claridge D. Generalization of the fourier series approach to model hourly energy use in commercial buildings. Trans ASME February 1999;121:54.
[19] Ji Ying, Xu Peng, Ye Yunyang. HVAC terminal hourly end-use disaggregation in commercial buildings with Fourier series model. Energy Build 2015;97:33–46.

[20] Zhou YP, Wu JY, Wang RZ, Shiochi S, Li YM. Simulation and experimental validation of the variable-refrigerant-volume (VRV) air-conditioning system in EnergyPlus. Energy Build 2008;40(6):1041–7.
[21] Al-ajmi FF, Hanby VI. Simulation of energy consumption for Kuwaiti domestic buildings. Energy Build 2008;40(6):1101–9.
[22] O'Neilla Zheng, Pang Xiufeng, Shashanka Madhusudana, Haves Philip, Bailey Trevor. Model-based real-time whole building energy performance monitoring and diagnostics. J Build Perform Simul 2014;7(2):83–99.
[23] Winkelmann F, Birdsall B, Buhl W. DOE-2 supplement: version 2.1 e. LBL-34947. Berkeley: Calif Lawrence Berkeley Lab; 1993.
[24] ESRU. ESP-r. [accessed 05.12.09.]. http://www.esru.strath.ac.uk/.
[25] USDE. 2009a. "EnergyPlus testing and validation, Department Energy, USA." [accessed 06.12.09]. http://apps1.eere.energy.gov/buildings/energyplus.
[26] Solar Energy Laboratory. TRNSYS version 17.02 user manual and documentation, solar energy laboratory, mechanical engineering department. Madison, WI: University of Wisconsin; May 2014.
[27] IEA ECBCS Annex 53, Annex 53 total energy use in buildings: analysis & evaluation methods, www.ecbcsa53.org.
[28] Energy Efficiency Verification Specialists, International Performance Measurement and Verification Protocol (IPMVP), 2002.
[29] ASHRAE. ASHRAE guideline 14–2002, measurement of energy and demand savings. 2002.
[30] Hensen Jan LM, Lamberts Roberto. Building performance simulation for design and operation. Published by Spon Press; 2011.
[31] Carroll WL, Hitchcock RJ. Tuning simulated building descriptions to match actual utility data: methods and implementation. ASHRAE Trans 1993;99:928–34.
[32] Lavigne Karine. Assisted calibration in building simulation–algorithm description and case studies. In: Eleventh International IBPSA Conference, Glasgow, Scotland; July 27-30, 2009.
[33] Wang Shengwei, Yan Chengchu, Xiao Fu. Quantitative energy performance assessment methods for existing buildings. Energy Build 2012;55:873–88.
[34] Karlsson F, Rohdin P, Persson ML. Measured and predicted energy demand of a low energy building: important aspects when using building energy simulation. Build Serv Eng Res Technol 2007;28:223–35.
[35] Turner C, Frankel M. Energy performance of LEED for new construction buildings. Washington, DC: New Buildings Institute; 2008.
[36] Scofield JH. Do LEED-certified buildings save energy? Not really…. Energy Build 2009;41:1386–90.
[37] Coakley Daniel, Raftery Paul, Keane Marcus. A review of methods to match building energy simulation models to measured data. Renew Sustain Energy Rev 2014;37:123–41.
[38] Pedrini A, Westphal FS, Lamberts R. A methodology for building energy modelling and calibration in warm climates. Build Environ 2002;37:903–12.
[39] Royapoor Mohammad. Tony Roskilly. Building model calibration using energy and environmental data. Energy Build 2015;94:109–20.
[40] Liu Simeng, Gregor P Henze. Calibration of building models for supervisory control of commercial buildings. In: Ninth International IBPSA Conference. Montréal, Canada; August 15-18, 2005.
[41] Agami Reddy T, Maor Itzhak. Procedures for reconciling computer-calculated results with measured energy data. ASHRAE Research Project 1051- RP. 2006.
[42] Raftery Paul, Keane Marcus, Costa Andrea. Calibrating whole building energy models: detailed case study using hourly measured data. Energy Build 2011;43:3666–79.
[43] Kandil Alaa-Eldin, Love James A. Signature analysis calibration of a school energy model using hourly data. J Build Perform Simul 2014;7(5):326–45.
[44] Zhao Jie, Lam Khee Poh, Ydstie B Erik, Karaguzel Omer T. EnergyPlus model-based predictive control within design–build–operate energy information modelling infrastructure. J Build Perform Simul 2015;8(3):121–34.
[45] Antonopoulos KA, Koronaki E. Envelope and indoor thermal capacitance of buildings. Appl Therm Eng 1999;19:743–56.
[46] Zhou Junli. Calculation of indoor air temperature and analysis of relative factors in natural ventilated buildings coupled with thermal mass. PhD thesis. Hunan University; 2009 [In Chinese].
[47] Handbook of fundamentals, American society of heating. Atlanta, USA: Refrigerating and Air-Conditioning Engineers; 2005.
[48] Emmerich SJ, Persily AK. Energy impacts of infiltration and ventilation in US office buildings using multizone airflow simulation. Proc IAQ Energy 1998;98:191–206.
[49] Wang Shengwei, Xu Xinhua. Parameter estimation of internal thermal mass of building dynamic models using genetic algorithm. Energy Convers Manag 2006;47:1927–41.
[50] Ng Lisa C, Persily Andrew K, Emmerich Steven J. Improving infiltration modeling in commercial building energy models. Energy Build 2015;88:316–23.